GEOPHYSICAL RESEARCH LETTERS, VOL. 25, NO. 3, PAGES 289-292, FEBRUARY 1, 1998

The correlation of AKR waves with precipitating electrons as determined by plasma wave and x-ray image data from the POLAR spacecraft

W. L. Imhof, D. L. Chenette, D. W. Datlowe, J. Mobilia

Lockheed Martin Palo Alto Research Laboratory, Palo Alto, California

M. Walt

STAR Laboratory, Stanford University, Stanford, California

R. R. Anderson

Department of Physics and Astronomy, University of Iowa, Iowa City

Abstract. Simultaneous measurements are presented of the intensities of AKR waves in the 60 kHz to 800 kHz range and the local time distributions of the fluxes of electrons precipitating into the atmosphere using wave and bremsstrahlung x-ray data acquired on the POLAR spacecraft. The images of 2 to 12 keV x-ray emission measured with the PIXIE spectrometer were used to obtain the positions and intensities of the electron precipitation regions. Electric field wave measurements of the AKR were obtained with the Plasma Wave Instrument (PWI). Data are presented from a satellite pass on 19 April 1996 in which there were several short term enhancements in the intensities of both waves and x-rays. The AKR electric field strengths were correlated with x-rays emitted over a six hour local time range in the pre-midnight sector with a correlation coefficient of 0.51. At the times of some of the rapid increases in the x-ray fluxes the AKR intensities exhibited similar sharp onsets.

Introduction

Auroral Kilometric Radiation (AKR) is an electromagnetic emission from approximately 30 kHz to several hundred kHz which is generated at auroral latitudes and propagates away from the earth. It is believed to be produced in cavities of low electron density by a cyclotron maser instability driven by an anisotropic, energetic electron distribution. This emission has been measured extensively by Gurnett (1974, 1983), Alexander and Kaiser (1976), Benson (1985), James (1980) and others. The association of AKR with bright auroral forms was made by Gurnett (1974) and by Benson and Akasofu (1984) and described with greater precision by Huff et al. (1988) who traced AKR generation sites to the field lines occupied by discrete auroral arcs. Benson and Calvert (1979) showed that AKR sources were on the same field lines as inverted V electron precipitation events. They also showed that AKR occurred at a frequency close to the electron gyrofrequency in regions of low ambient electron density. The cyclotron maser process itself has been described by Wu and Lee (1979), Calvert (1982), and others. A recent review of auroral region waves including AKR has been published by Andre (1997).

Later satellite missions have flown near or in regions of AKR generation (e.g. Bahnsen et al., 1989; Roux et al., 1993). These source regions were identified primarily by the strong AKR radiation at a frequency near the local electron gyrofrequency. In agreement with theory these regions also exhibited a low ambient electron density and an anisotropic energetic electron distribution. Source regions have been found between 18:00 Magnetic Local Time (MLT) and 06:00 MLT. With only local measurements available it has not been possible to survey the entire auroral oval at one time to determine the longitudinal extent of maser action.

Inverted V structures accelerate electrons into the atmosphere producing auroral luminosity and bremsstrahlung x-rays. Thus, it is expected that x-ray production regions will correspond to locations of AKR generation. Since images of x-ray sources from the entire polar area can now be obtained by satellite, it is of interest to examine whether these images also map out the sites of AKR generation. However, the relationship of bremsstrahlung x-rays and AKR must first be established. In this paper we examine simultaneous records of AKR and auroral bremsstrahlung x-ray images to investigate the relationship of these emissions.

Simultaneous measurements of AKR intensities and auroral x-rays were performed with instruments on the POLAR satellite. The x-ray images were obtained with the PIXIE x-ray spectrometer, a multiple pinhole x-ray camera designed to image the entire auroral region from high altitude (Imhof et al, 1995). With x-ray data available for the entire polar cap, irrespective of solar illumination, this comparison can be done as a function of the local time of the x-ray production site. The electric field wave data used in this study were acquired with the Plasma Wave Instrument (PWI) Sweep Frequency Receiver (SFR) connected to a long electric dipole antenna with a sphere-to-sphere separation of 130 m (Gurnett et al., 1995). To demonstrate the type of information that can be derived from these data, we present x-ray and AKR intensities obtained during one high altitude pass of the POLAR satellite.

Paper number 97GL03770.
0094-8534/98/97GL-03770$05.00

Presentation Of Data

Between 20 March 1996 and 1 April 1997, all north polar passes of the POLAR satellite were visually surveyed at times when the PIXIE instrument was outside the radiation belts and in full operation. Time periods were selected when strong auroral x-ray fluxes and intense AKR were present. To associate x-ray regions with AKR, attention was given to cases in which significant time variations in both x-rays and AKR occurred so that the time variations could be correlated. Since the PIXIE instrument was operated intermittently and data were analyzed only when there were significant enhancements in both the AKR waves and the x-ray fluxes, the quantity of data processed in this investigation was quite limited.

An example of simultaneous x-ray and plasma wave data is shown in Figure 1. In the upper section an image of 2 to 12 keV x-rays is displayed. The terminator is shown by the

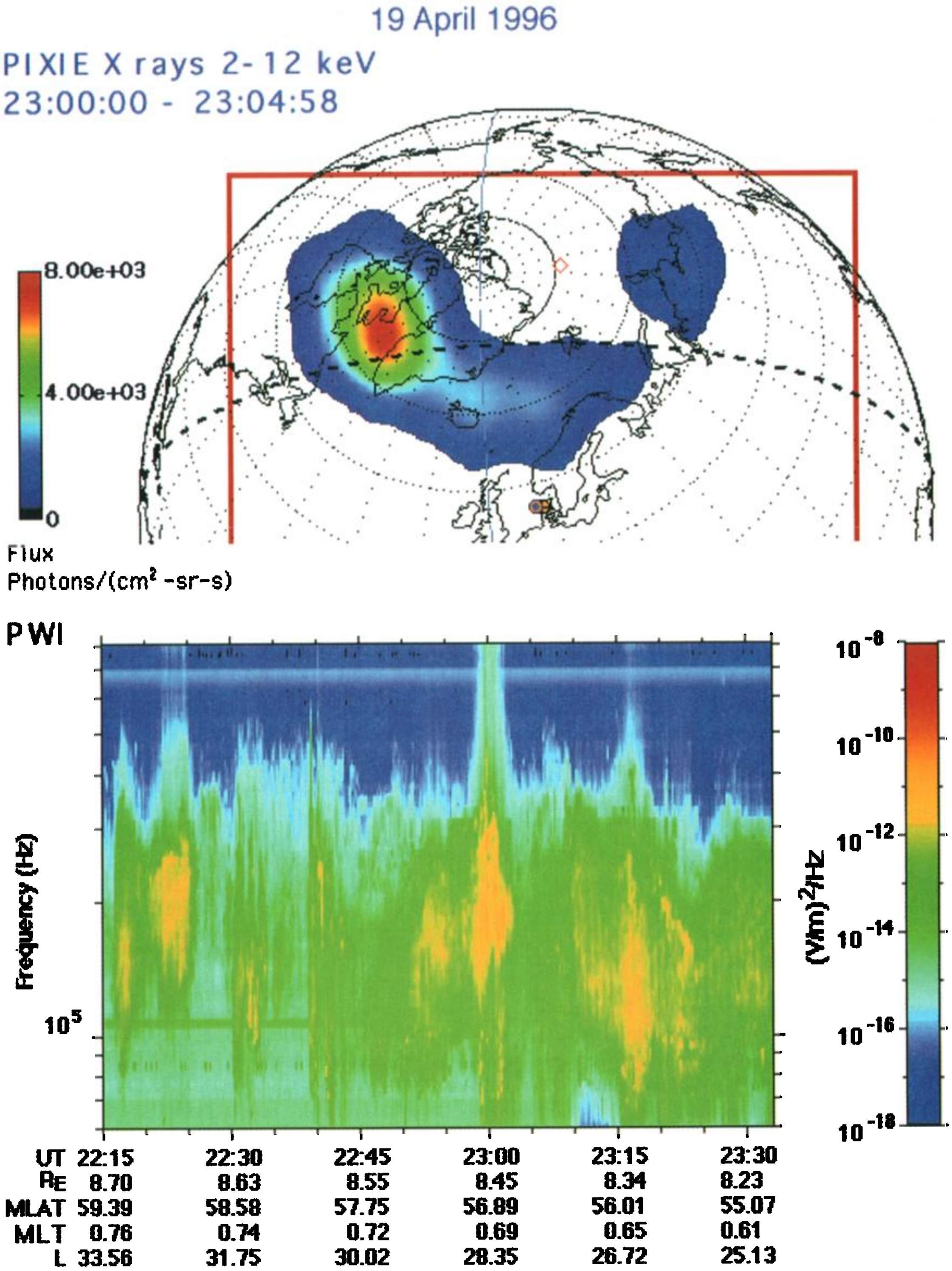

Figure 1. Upper section : an x-ray image 2 to 12 keV accumulated from 22:59:30 to 23:04:30 UT. Lower section: an electric field spectrogram from the Sweep Frequency Receiver A in PWI.

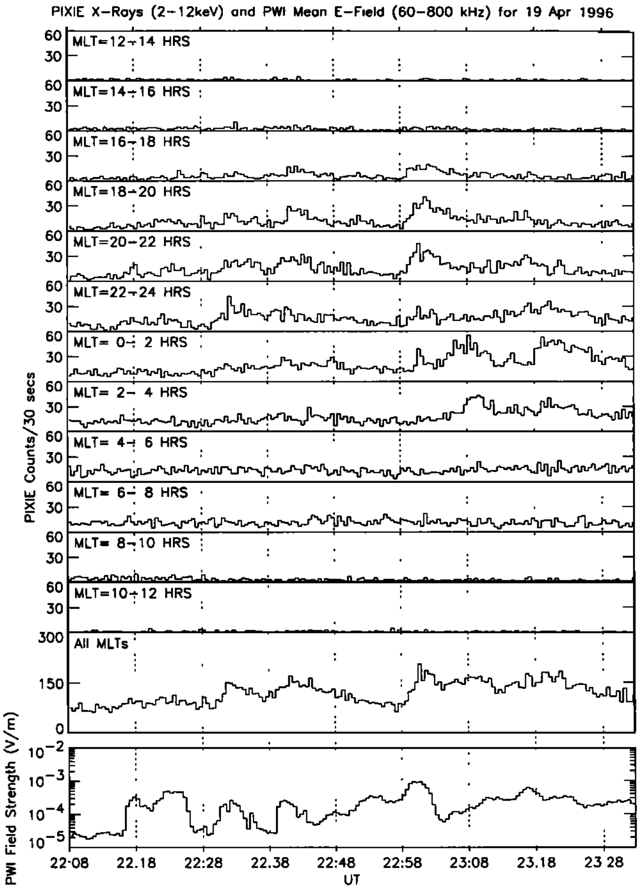

Figure 2. Counting rates of x-rays in successive two hour MLT intervals. The next to bottom panel shows x-ray counts accumulated at all MLT whereas the mean value of the AKR electric field strength is plotted in the bottom section.

dashed line and illustrates the ability of the x-ray camera to measure electron precipitation in daylight as well as at night. The lower section is a 1 hr. 20 min. spectrogram of the PWI electric field wave intensity between 60 kHz and 800 kHz. The x-ray image corresponds to a time (≈23:00 UT) of intense AKR. Although several examples showing similar time variations of AKR and x-rays have been found, this case was selected for detailed study because the time interval contained several pronounced enhancements in both x-rays and AKR.

The x-ray counts and AKR electric field strengths are plotted together in Figure 2 for the time period 22:08 to 23:33 UT, 19 April 1996. The PIXIE counts assigned to each 2 hr MLT sector are the number of detected x-rays which originated during each 30 s segment. X-ray background in PIXIE is negligible during this time as is apparent from the few counts recorded in the 10-12 hr MLT sector or outside the auroral oval in Figure 1. Note that the x-ray-counts are plotted on a linear intensity scale while the AKR intensities are on a logarithmic scale as the dynamic range of the electric field intensity is much larger. The AKR electric field strengths are derived from integrating the intensity over the bandwidth of the emission, 60 kHz to 800 kHz.

In Figure 3 the correlation coefficients between the AKR mean electric field strengths and x-ray counts are plotted as a function of the MLT of the x-ray emitting region in two hour MLT intervals. Clearly, during this orbit the correlation is

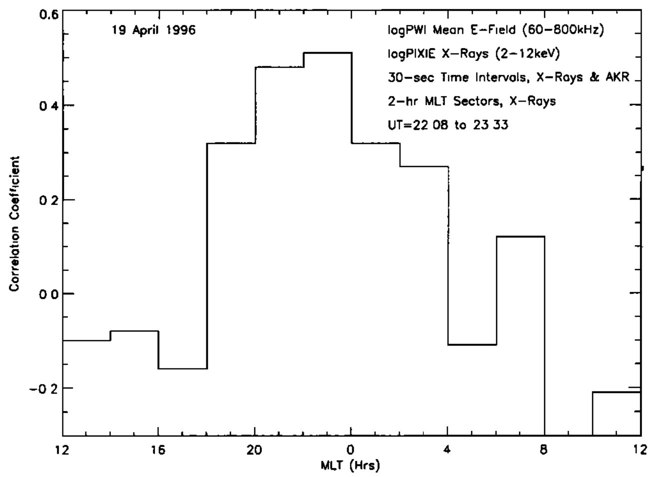

Figure 3. The correlation coefficient between AKR and 2 to 12 keV x-rays as a function of MLT.

higher in the pre-midnight region than at other local times. For the three 2 hr sectors before midnight the correlation coefficients between the logarithm of the AKR intensity and the logarithm of the x-ray flux were 0.32, 0.48, and 0.51 and the statistical significance was 4.5, 7.2, and 7.7. The statistical significance is the number of standard deviations by which the correlation coefficient exceeds zero, assuming the two quantities being compared are linearly related (Hoel, 1947). Although some correlation coefficients larger than 0.51 were obtained in the analysis of other orbits (not shown here), this case was selected for presentation because several narrow time enhancements were observed and the time period exceeded one hour.

In Figure 4 the AKR wave intensities are plotted with the counts of x-rays emitted from the 18 to 24 hr MLT interval, which exhibited a strong correlation with a high statistical accuracy. With a logarithmic value for each quantity the coefficient for this MLT interval is 0.51 with a probable error of 0.02 due to the statistical uncertainties in the numbers of x-ray counts. For linear values of the AKR and x-ray fluxes the correlation coefficient is 0.46 with a probable error of 0.02. Again the significance of the correlation is very high. The dependence of the correlation coefficient on the AKR wave

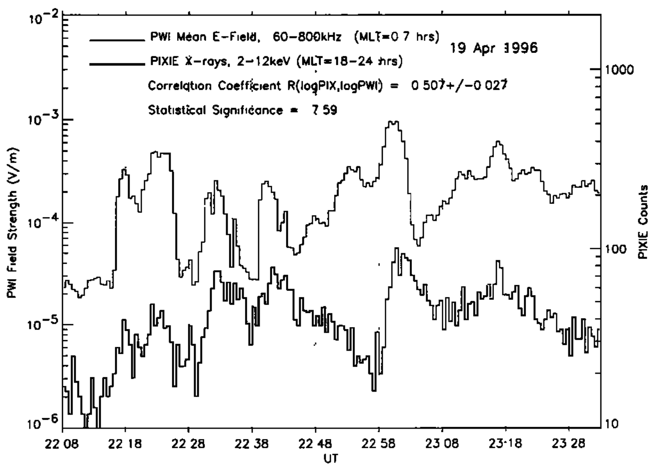

Figure 4. Comparison between AKR electric field and PIXIE x-rays emitted from the MLT region 18 to 24 hrs as a function of UT.

mode is not available since the polarization of the AKR could not be measured this time by PWI due to selected antennas.

For the orbit analyzed the AKR intensities have a higher correlation with the precipitation fluxes in the pre-midnight region than at other local times. Several of the abrupt increases in AKR match closely in time the rapid increases in x-ray counting rates. Although the reliability of the correlation coefficient is high the correlation coefficient of 0.51 indicates that only about 25% of the variance in the AKR or x-ray intensity can be accounted for by a relationship with the other quantity. The remainder of the variance may be attributed to 1) AKR produced by electrons with energies too low to produce > 2 keV x-rays, 2) AKR produced at local times not included in the 6 hour sector of MLT, 3) propagation effects in which the AKR waves did not reach the location of POLAR, and 4) production of AKR by trapped particle anisotropies which do not lead to strong precipitation. The validity of 1) could be checked by examination of the output from the other POLAR imagers (VIS and UVI) that are sensitive to low energy electrons, but these instruments were not operating at the time. For future analysis of other POLAR data the outputs of these instruments can be used for this purpose. Such data might also establish the occurrence of auroral arcs with the existence of AKR. From the x-ray counts in Figure 2 it is apparent that only about half of the x-rays originate in the 18-24 hr MLT interval. Therefore, it is not surprising that the overall correlation coefficient is not high although the long sequence of data pairs leads to a high confidence of correlation.

The ability to monitor electron precipitation over the entire polar cap with PIXIE at the same time that AKR is recorded opens several possibilities for the study of AKR generation. In particular the PIXIE ability to measure x-ray spectra will allow an assessment of the precipitating electron energy spectra and therefore the characteristics of the electron fluxes associated with AKR. A recent suggestion by Calvert (1995) that the AKR may trigger electron precipitation can, in principle, be tested by detailed comparisons of the sudden, almost simultaneous increases in AKR and x-rays illustrated in Figure 4. Other important topics suitable for investigation are the following:

- The local time dependence of AKR generation during the course of magnetic substorms.
- The dependence of AKR frequency (altitude of generation) and intensity on the energy spectrum of the precipitating electrons.
- Comparison of the time profiles of AKR bursts and precipitating electron enhancements.

Summary

This investigation represents the first comparison of global-scale electron precipitation, as determined from bremsstrahlung emission, with the intensity of AKR waves. On 19 April 1996 good correlations between AKR and x-rays were observed with the largest ones being in the 18 to 24 MLT sector. Most of the abrupt changes in x-ray intensity in the 18 to 24 MLT interval were associated with similar AKR intensity changes. However, the moderately strong correlation coefficient, while highly significant statistically, indicates that other factors also influence the x-rays and AKR reaching POLAR.

Acknowledgments. The PIXIE data analysis was supported by NASA contract NAS-5-30372 from GSFC. The PWI analysis was conducted under contract NAS-5-30371. At Lockheed Martin we wish to thank John Hawley and Michael Rinaldi for their contribution to the data analysis. At the University of Iowa we wish to thank Julie Dowell for her programming effort.

References

Alexander, J. K., and M. L. Kaiser, Terrestrial Kilometric Radiation 1. Spatial Structure Studies, J. Geophys. Res., 81, 5948-5956, 1976.

Andre, M., Waves and wave-particle interactions in the auroral region, J. Atmos. Solar-Terrestrial Phys., 59, 1687, 1997.

Bahnsen, A., B. M. Pedersen, M. Jespersen, E. Ungstrup, L. Eliasson, J. S. Murphree, R. D. Elphinstone, L. Blomberg, G. Holmgren, and L. J. Zanetti, Viking observations at the source region and auroral kilometric radiation, J. Geophys. Res., 94, 6643, 1989.

Benson, R. F., and W. Calvert, ISIS-1 observations at the source of auroral kilometric radiation, Geophys. Res. Lett., 6, 479-482, 1979.

Benson, R. F., and S.-I. Akasofu, Auroral kilometric radiation/aurora correlation, Radio Sci., 19, 527, 1984

Benson, R. F., Auroral kilometric radiation: Wave modes, harmonics and source region electron density structures, J. Geophys. Res., 90, 2753, 1985.

Calvert, W., A feedback model for the source of auroral kilometric radiation, J. Geophys. Res., 87, 8199, 1982.

Calvert, W., An explanation for auroral structure and the triggering of auroral kilometric radiation, J. Geophys. Res. 100, 14887, 1995.

Gurnett, D. A., The earth as a radio source: Terrestrial kilometric radiation., J. Geophys. Res., 79, 4227, 1974.

Gurnett, D. A., High latitude electromagnetic plasma wave emissions in high latitude space plasma physics, edited by B. Hultqvist and T. Hagfors, p. 355, Plenum, New York, 1983.

Gurnett, D. A., A. M. Persoon, R. F. Randall, D. L. Odem, S. L. Remington, T. F. Averkamp, M. M. Debower, G. B. Hospodarsky, R. L. Huff, D. L. Kirchner, M. A. Mitchell, B. T. Pham, J. R. Phillips, W. J. Schintler, P. Sheyko, and D. R. Tomas, The POLAR plasma wave instrument, Space Science Reviews 71: 597-622, 1995.

Hoel, P. G. Introduction to mathematical statistics, pp 81-89, John Wiley and sons, N.Y., 1947.

Huff, R. L., W. Calvert, J. D. Craven, L. A. Frank, and D. A. Gurnett, Mapping of auroral kilometric radiation sources to the aurora, J. Geophys. Res., 93, 11445, 1988.

Imhof, W. L., K. A. Spear, J. W. Hamilton, B. R. Higgins, M. J. Murphy, J. G. Pronko, R. R. Vondrak, D. L. McKenzie, C. J. Rice, D. J. Gorney, D. A. Roux, R. L. Williams, J. A. Stein, J. Bjordal, J. Stadsnes, K. Njoten, T. J. Rosenberg, L. Lutz and D. Detrick, The POLAR ionospheric x-ray imaging experiment (PIXIE), Space Science Reviews 71: 385-408, 1995.

James, H. G., Direction-of-arrival measurements of auroral kilometric radiation and associated ELF data from ISIS 1, J. Geophys. Res., 85, 3367, 1980.

Roux, A., A. Hilgers, H. DeFraudy, D. LeQueau, P. Louran, S. Perraut, A. Bahnsen, M. Jespersen, E. Ungstrup, and M. Andre, Auroral kilometric radiation sources in situ and remote observations from Viking, J. Geophys. Res., 98, 11657-11670, 1993.

Wu, C.S., and L. C. Lee, A theory of the terrestrial kilometric radiation, Astrophys. J., 230, 621-626, 1979.

R.R. Anderson, Department of Physics and Astronomy, University of Iowa, Iowa City, IA 52242.

D.L. Chenette, D.W. Datlowe, W.L. Imhof, and J. Mobilia, Lockheed Martin Palo Alto Research Laboratory, Palo Alto, CA 94304.

M. Walt, STARLAB, Stanford University, Stanford, CA 94305.

(Received July 18, 1997; revised December 5, 1997; accepted December 17, 1997.)